

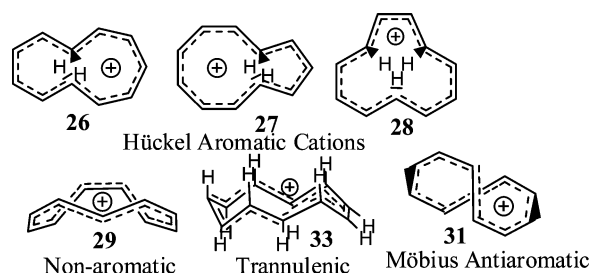
## Aromaticity and Möbius Antiaromaticity in Monocyclic [11]Annulenium Cations

Philip M. Warner

Department of Chemistry and Chemical Biology, Northeastern University, Boston, Massachusetts 02115

p.warner@neu.edu

Received June 5, 2006



Monocyclic [11]annulenium cations, which are experimentally unknown, have been studied primarily via DFT methods but also with some CCSD(T) validation. We have located six minima: two doubly *trans* (**26**, **27**), one triply *trans* (**28**), one singly *trans* (**29**), one quintuply *trans* (trannulene-type, **33**), and one all-*cis* (**31**). The first three are aromatic, **33** is modestly aromatic, **29** is nonaromatic, and the last is a Möbius antiaromatic species. We also investigated the fusion of various numbers of three-membered rings (3MRs) to the central 11-membered ring (11MR). We found several planar, all-*cis*-[11]annulenium ion derivatives as well as another Möbius antiaromatic species (**52b**); for comparison, we also found planar, antiaromatic all-*cis*-[12]annulene (**60**) and [15]annulenium cation (**61**) derivatives. The (anti)-aromatic characterization of these compounds is based mainly on calculated magnetic data for the ground singlet and vertical triplet states, although aromatic stabilization energies (ASE) are also considered. Data for optimized triplets, several of which are Möbius aromatic systems (**31t**, **52t**, **63t**, **64t**), are also included. Several of these cations are reasonable synthetic targets.

### Introduction

The history of medium-ring monocyclic annulenes is replete with experimental and theoretical difficulties.<sup>1</sup> Masamune completed a long and complex saga of work aimed at establishing the aromaticity of [10]annulene.<sup>2</sup> Because of steric strain in the di-*trans* (**1**) and all-*cis* (**2**) isomers, the assignment of aromaticity to the highly unstable species involved is problematic. Theoretical work was also difficult,<sup>3</sup> particularly because DFT methods apparently gave the wrong energy ordering of the various possible [10]annulene isomers.<sup>4</sup> On the basis of CCSD(T) calculations by Schaefer,<sup>5</sup> it is now agreed that the coiled (twisted),

$C_2$  stereoisomer is the most stable, followed by the  $C_2$  di-*trans*, naphthalene-like shaped stereoisomer. A “heart-shaped” mono-*trans* isomer (**3**), calculated to be the most stable by DFT,<sup>5b</sup> is now understood to be less stable than the aforementioned two. However, Schleyer et al.<sup>6</sup> have calculated that fusion of just two three-membered rings (3MRs) to the [10]annulene skeleton would lead to a stable, planar, aromatic  $D_{2h}$  all-*cis* structure (**4**) [as judged by energetic (aromatic stabilization energy, ASE) and magnetic criteria, including magnetic susceptibility exaltation (MSE) and NICS]; the large external cyclopropene angles enable the stability of the planar structure. Fusion of five 3MRs leads to the prediction of a stable, planar  $D_{5h}$  structure (**5**).

In contrast to the relatively extensive consideration given to [10]annulenes (including the extensive work on bridged [10]-annulenes initiated by Vogel),<sup>7</sup> [11]annulenium cations (monocyclic) and [12]annulenes (monocyclic) have been much less

(1) Wiberg, K. B. *Chem. Rev.* **2001**, *101*, 1317.

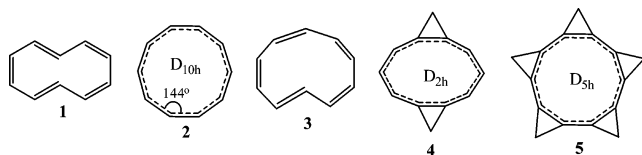
(2) (a) Masamune, S.; Hojo, K.; Bigam, G.; Raberstein, D. L. *J. Am. Chem. Soc.* **1971**, *93*, 4966. (b) Masamune, S.; Darby, N. *Acc. Chem. Res.* **1972**, *5*, 272.

(3) (a) Castro, C.; Karney, W. L.; McShane, C. M.; Pemberton, R. P. *J. Org. Chem.* **2006**, *71*, 3001. (b) Sulzbach, H. M.; Schleyer, P. v. R.; Jiao, H.; Xie, Y.; Schaefer, H. F. *J. Am. Chem. Soc.* **1995**, *117*, 1369. (c) Xie, Y.; Schaefer, H. F.; Liang, G.; Bowen, J. P. *J. Am. Chem. Soc.* **1994**, *116*, 1442.

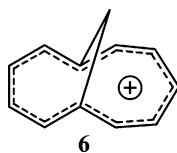
(4) See, however: Wannere, C. S.; Sattelmeyer, K. W.; Schaefer, H. F.; Schleyer, P. v. R. *Angew. Chem., Int. Ed.* **2004**, *43*, 4200.

(5) (a) King, R. A.; Crawford, T. D.; Stanton, J. F.; Schaefer, H. F. *J. Am. Chem. Soc.* **1999**, *121*, 10788. (b) Sulzbach, H. M.; Schaefer, H. F.; Klopper, W.; Lüthi, H. P. *J. Am. Chem. Soc.* **1996**, *118*, 3519.

(6) Schleyer, P. v. R.; Jiao, H.; Sulzbach, H. M.; Schaefer, H. F. *J. Am. Chem. Soc.* **1996**, *118*, 2093.



studied. To be sure, a variety of dehydro[12]annulenes have been studied, both experimentally<sup>8</sup> and theoretically,<sup>9</sup> but the parent [12]annulene, synthesized photochemically at low temperature (apparently, only the tri-*trans* stereomer) and studied briefly,<sup>10</sup> has only recently been studied with modern theoretical methods.<sup>11</sup> Among the myriad of possible [11]annulenium cations, only the bridged 1,6-methano[11]annulenium cation, **6**, appears to have been prepared<sup>12</sup> or even discussed.



In this paper, we present theoretical results for various monocyclic [11]annulenium cations, including ones containing fused 3MRs. We also cover a few other annulene species with fused 3MRs.

### Computational Methodology

All structures were optimized at the B3LYP/6-31G\* level of theory,<sup>13</sup> followed by frequency calculations at the same level to determine the nature of the optimized structures (i.e., number of imaginary frequencies (Nimag): 0 for minima, 1 for transition states, etc.) and to obtain zero-point energies (unscaled) and thermochemical corrections. Full details of these are given in the Supporting Information. Diamagnetic susceptibilities, in centimeter-gram-second parts per million ( $\chi$ ), were calculated using the

(7) Vogel, E. *Spec. Publ. Chem. Soc.* **1967**, 21, 113. SciFinder Scholar now lists 217 publications on bridged [10]annulenes.

(8) Recent interest has centered on optoelectronic properties and carbon allotrope precursors: (a) Gard, M. N.; Kiesewetter, M. K.; Reiter, R. C.; Stevenson, C. D. *J. Am. Chem. Soc.* **2005**, 127, 16143. (b) Mittelz, F.; Boudon, C.; Gisselbrecht, J.-P.; Gross, M.; Diederich, F. *Chem. Commun.* **2002**, 2318. (c) Marsella, M. J. *Acc. Chem. Res.* **2002**, 35, 944. (d) Iyoda, M.; Vorasingha, A.; Kuwatani, Y.; Yoshida, M. *Tetrahedron Lett.* **1998**, 39, 4701. (e) Haley, M. M.; Brand, S. C.; Pak, J. J. *Angew. Chem., Int. Ed. Engl.* **1997**, 36, 835. (f) Anthony, J.; Boldi, A. M.; Boudon, C.; Gisselbrecht, J.-P.; Gross, M.; Seiler, P.; Knobler, C. B.; Diederich, F. *Helv. Chim. Acta* **1995**, 78, 797. (g) Anthony, J.; Knobler, C. B.; Diederich, F. *Angew. Chem., Int. Ed. Engl.* **1993**, 32, 406. For earlier work, see: (h) Sondheimer, F.; Wolovsky, R.; Garratt, P. J.; Calder, I. C. *J. Am. Chem. Soc.* **1966**, 88, 2610. (i) Untch, K. G.; Wysocki, D. C. *J. Am. Chem. Soc.* **1966**, 88, 2608. (j) Wolovsky, R.; Sondheimer, F. *J. Am. Chem. Soc.* **1965**, 87, 5720.

(9) Juselius, J.; Sundholm, D. *Phys. Chem. Phys.* **2001**, 3, 2433. (10) (a) Gard, M. N.; Reiter, R. C.; Stevenson, C. D. *Org. Lett.* **2004**, 6, 393 (synthesis of a di-*trans*-[12]annulene reported). (b) Stevenson, G. R.; Concepcion, R.; Reiter, R. C. *J. Org. Chem.* **1983**, 48, 2777. (c) Oth, J. F. M. *Pure Appl. Chem.* **1971**, 25, 573. (d) Oth, J. F. M.; Gilles, J. M.; Schröder, G. *Tetrahedron Lett.* **1970**, 67. (e) Oth, J. F. M.; Röttele, H.; Schröder, G. *Tetrahedron Lett.* **1970**, 61.

(11) (a) Castro, C.; Karney, W. L.; Valencia, M. A.; Vu, C. M. H.; Pemberton, R. P. *J. Am. Chem. Soc.* **2005**, 127, 9704. (b) Castro, C.; Karney, W. L.; Vu, C. M. H.; Burkhardt, S. E.; Valencia, M. A. *J. Org. Chem.* **2005**, 70, 3602. (c) Castro, C.; Isborn, C. M.; Karney, W. L.; Mauksch, M.; Schleyer, P. v. R. *Org. Lett.* **2002**, 4, 3431.

(12) (a) Destro, R.; Simonetta, M. *Acta Cryst., Sect. B* **1979**, 35, 1846. (b) Haddon, R. C. *J. Org. Chem.* **1977**, 42, 2017. (c) Destro, R.; Pilati, T.; Simonetta, M. *J. Am. Chem. Soc.* **1976**, 98, 1999. (d) Kemp-Jones, A. V.; Jones, A. J.; Sakai, M.; Beeman, C. P.; Masamune, S. *Can. J. Chem.* **1973**, 51, 767. (e) Vogel, E.; Feldmann, R.; Duewel, H. *Tetrahedron Lett.* **1970**, 1941. (f) Grimm, W.; Hoffmann, H.; Vogel, E. *Angew. Chem.* **1965**, 77, 348.

continuous set of gauge transformations method (CSGT/B3LYP/6-311+G\*\*)<sup>14</sup>; the larger basis set is necessary to get reasonably accurate results. NICS (ppm) calculations<sup>15</sup> were performed using the gauge independent atomic orbitals method (GIAO/B3LYP/6-31+G\*\*).<sup>16</sup> For planar species, the ghost atom (Bq) was placed at the ring center, the standard NICS location (NICS[0]). For nonplanar species, several locations were studied; the NICS[0] location is the one reported because variance in the values at NICS[1] and similar locations was small enough to not effect any conclusions.<sup>17</sup> In addition, the calculated magnetic shieldings of the actual atoms are often indicative of the electronic structure and are presented where appropriate. Because DFT can overemphasize the energetic worth of delocalization and has thus produced the wrong energy ordering among some of the [10]annulenes,<sup>5a</sup> all stationary points of the formula  $C_{11}H_{11}^+$  were recomputed at the CCSD(T)/6-31G\*\*//B3LYP/6-31G\* level.<sup>18</sup> All calculations were carried out using the Gaussian 98<sup>19</sup> or 03<sup>20</sup> suite of programs.

**Models for Aromatic Stabilization Energies (ASEs) and Magnetic Susceptibility Exaltations ( $\Lambda$ ).** Because the systems studied here are all medium-ring compounds, they suffer from varying amounts of strain energy, which must be factored out to obtain reasonably accurate ASEs. As pointed out by Schleyer,<sup>6</sup> this may be achieved by constraining the bond angles of model polyenic compounds to be the same as those for the actual molecule for which the ASE is being calculated. Then, the procedure just requires model compounds with the same kinds of bonds as the target “parent” compound, and one gets the “strain-corrected” ASE via

(13) (a) Becke, A. D. *J. Chem. Phys.* **1993**, 98, 5648. (b) Becke, A. D. *J. Chem. Phys.* **1993**, 98, 1372. (c) Lee, C.; Yang, W.; Parr, R. G. *Phys. Rev. B* **1988**, 37, 785. (d) Stephens, P. J.; Devlin, F. J.; Chabalowski, C. F.; Frisch, M. J. *J. Phys. Chem.* **1994**, 98, 11623.

(14) (a) Jiao, H. J.; Schleyer, P. v. R. *Angew. Chem., Int. Ed. Engl.* **1995**, 34, 334. (b) The CSGT method: Keith, T. A.; Bader, R. W. F. *Chem. Phys. Lett.* **1993**, 210, 223.

(15) (a) Schleyer, P. v. R.; Maerker, C.; Dransfeld, A.; Jiao, H. J.; Hommes, N. J. R. v. E. *J. Am. Chem. Soc.* **1996**, 118, 6317. (b) Schleyer, P. v. R.; Manoharan, M.; Wang, Z.-X.; Kiran, B.; Jiao, H.; Puchta, R.; Hommes, N. J. R. v. E. *Org. Lett.* **2001**, 3, 2465.

(16) (a) Dodds, J. L.; McWeeny, R.; Sadlej, A. J. *Mol. Phys.* **1980**, 41, 1419. (b) Wolinski, K. J.; Hilton, F.; Pulay, P. *J. Am. Chem. Soc.* **1990**, 112, 8251.

(17) See, however: Stanger, A. *J. Org. Chem.* **2006**, 71, 883.

(18) (a) Bartlett, R. J. *J. Phys. Chem.* **1989**, 93, 1697. (b) Raghavachari, K.; Trucks, G. W.; Pople, J. A.; Head-Gordon, M. *Chem. Phys. Lett.* **1989**, 157, 479. (c) Scuseria, G. E. *Chem. Phys. Lett.* **1991**, 176, 27.

(19) Frisch, M. J.; Trucks, G. W.; Schlegel, H. B.; Scuseria, G. E.; Robb, M. A.; Cheeseman, J. R.; Zakrzewski, V. G.; Montgomery, J. A., Jr.; Stratmann, R. E.; Burant, J. C.; Dapprich, S.; Millam, J. M.; Daniels, A. D.; Kudin, K. N.; Strain, M. C.; Farkas, O.; Tomasi, J.; Barone, V.; Cossi, M.; Cammi, R.; Mennucci, B.; Pomelli, C.; Adamo, C.; Clifford, S.; Ochterski, J.; Petersson, G. A.; Ayala, P. Y.; Cui, Q.; Morokuma, K.; Malick, D. K.; Rabuck, A. D.; Raghavachari, K.; Foresman, J. B.; Cioslowski, J.; Ortiz, J. V.; Stefanov, B. B.; Liu, G.; Liashenko, A.; Piskorz, P.; Komaromi, I.; Gomperts, R.; Martin, R. L.; Fox, D. J.; Keith, T.; Al-Laham, M. A.; Peng, C. Y.; Nanayakkara, A.; Gonzalez, C.; Challacombe, M.; Gill, P. M. W.; Johnson, B. G.; Chen, W.; Wong, M. W.; Andres, J. L.; Head-Gordon, M.; Replogle, E. S.; Pople, J. A. *Gaussian 98*; Gaussian, Inc.: Pittsburgh, PA, 1998.

(20) Frisch, M. J.; Trucks, G. W.; Schlegel, H. B.; Scuseria, G. E.; Robb, M. A.; Cheeseman, J. R.; Montgomery, J. A., Jr.; Vreven, T.; Kudin, K. N.; Burant, J. C.; Millam, J. M.; Iyengar, S. S.; Tomasi, J.; Barone, V.; Mennucci, B.; Cossi, M.; Scalmani, G.; Rega, N.; Petersson, G. A.; Nakatsuji, H.; Hada, M.; Ehara, M.; Toyota, K.; Fukuda, R.; Hasegawa, J.; Ishida, M.; Nakajima, T.; Honda, Y.; Kitao, O.; Nakai, H.; Klene, M.; Li, X.; Knox, J. E.; Hratchian, H. P.; Cross, J. B.; Bakken, V.; Adamo, C.; Jaramillo, J.; Gomperts, R.; Stratmann, R. E.; Yazyev, O.; Austin, A. J.; Cammi, R.; Pomelli, C.; Ochterski, J. W.; Ayala, P. Y.; Morokuma, K.; Voth, G. A.; Salvador, P.; Dannenberg, J. J.; Zakrzewski, V. G.; Dapprich, S.; Daniels, A. D.; Strain, M. C.; Farkas, O.; Malick, D. K.; Rabuck, A. D.; Raghavachari, K.; Foresman, J. B.; Ortiz, J. V.; Cui, Q.; Baboul, A. G.; Clifford, S.; Cioslowski, J.; Stefanov, B. B.; Liu, G.; Liashenko, A.; Piskorz, P.; Komaromi, I.; Martin, R. L.; Fox, D. J.; Keith, T.; Al-Laham, M. A.; Peng, C. Y.; Nanayakkara, A.; Challacombe, M.; Gill, P. M. W.; Johnson, B.; Chen, W.; Wong, M. W.; Gonzalez, C.; Pople, J. A. *Gaussian 03*, revision B.04; Gaussian, Inc.: Wallingford, CT, 2004.

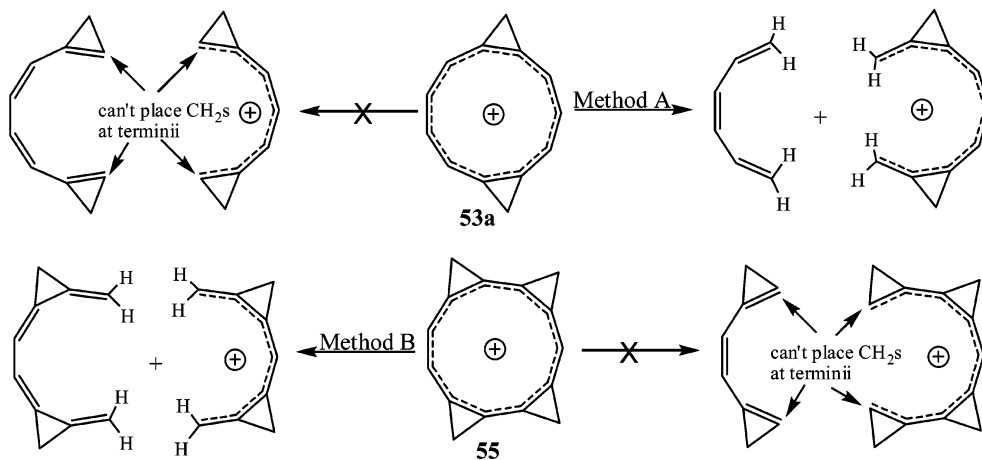
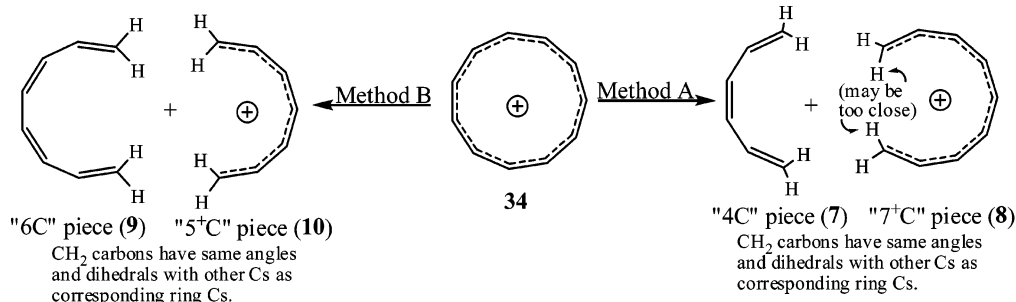
the appropriate homodesmotic equation. However, because types of bonds are rarely matched exactly, there is room for the introduction of errors. The more, and consequently smaller, model compounds, the greater the potential for errors. However, larger, and fewer, model compounds may have other shortcomings, such as particularly close distances between H's in planar systems.

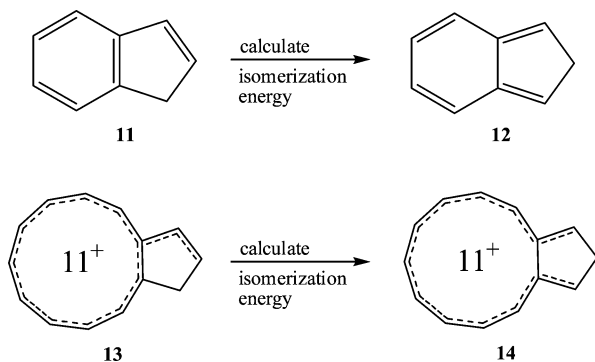
The problem becomes greater for charged systems because then charge delocalization as a stabilizing influence has to be factored out to get accurate ASEs (note that this is *not a concern with respect to magnetic properties*). For this reason, relatively large, charge-delocalized models are desirable. For this study, we have chosen to divide any given cyclic compound into only two pieces. For the [11]annulene cations, two choices are generally available, as shown below. Method A is to divide the ring into a 7C positive ion with a CH<sub>2</sub> at each end of the ion (to give a 9C cation model overall) and a 4C neutral piece with a CH<sub>2</sub> at each end (to give a 6C neutral model overall). All of the carbons are placed at the same position they occupy in the original ring (including the CH<sub>2</sub>), and all of their angles and dihedral angles are frozen. After optimization of all other parameters (B3LYP/6-31G\*), the energetic sum of the two pieces, minus twice the energy of ethylene (CH<sub>2</sub>=CH<sub>2</sub>) bonds, gives a calculated "nonaromatic" energy for the target compound; the difference between this value and the actual calculated value is the ASE (see eqs 1 and 3). For each model compound, the magnetic susceptibility was also calculated, and the same procedure as that above yields the MSE ( $\Lambda$ ; see eqs 2 and 4). The disadvantages of method A are (a) charge delocalization over a maximum of nine carbons, rather than the 11 of the parent carbocation, and (b) that the inner hydrogens of the CH<sub>2</sub>'s may be too close; both factors

raise the energy of the model and consequently enhance the ASE. Method B, in which the ring is divided into a 5C cation (+2 CH<sub>2</sub>'s) and a 6C neutral (+2 CH<sub>2</sub>'s), does not usually suffer from close approach of the hydrogens (26 and 27 are examples of exceptions) but does not have sufficient charge delocalization; this may serve to raise the apparent ASE even more. As will be seen, the results are mainly consistent with these expectations. Where possible, method A was used; for some (e.g., 26, 53a, 62), method B is not possible. However, in some 3MR fused cases, only method B can be employed, as shown below.

For the [10]annulene systems, method C involves division of the ring into a 6C and a 4C piece. For [12]annulenes, method D requires division of the ring into two 6C pieces. For the [9]-annulene cation, method E involves division of the ring into a 5C cationic piece and a 4C neutral piece. Last, for the [15]-annulene cation, method F is to divide the ring into a 9C cationic piece and a 6C neutral. In all cases, a CH<sub>2</sub> is added to each end of the ring fragments.

An (albeit expensive) alternative to the above fragment model method is to use the latest isomerization energy method (ISE<sub>II</sub>; herein called ISE2) of Schleyer.<sup>21</sup> This approach requires, for example, the calculation of the isomerization energy of indene (11, aromatic) to isoindene (12, nonaromatic); a correction for the two *cis*-butadiene to *trans*-butadiene subunits must also be applied (and this correction is angle dependent). When applied to charged systems (e.g., 13 to 14), the loss of aromaticity and possible differences in charge delocalization have to be considered. In addition, the nonplanar ions have unequal charge delocalizations and may not be able to delocalize charge into the 5MR (and this





may well be a function of where the 5MR is fused and what distortion the 5MR induces—the authors of the method used induced planarity in their studies). This method cannot be applied to all of the 3MR fused cases.

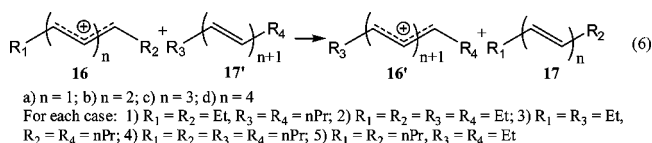
## Results and Discussion

### A. Evaluation of Aromatic Stabilization Energy (ASE)

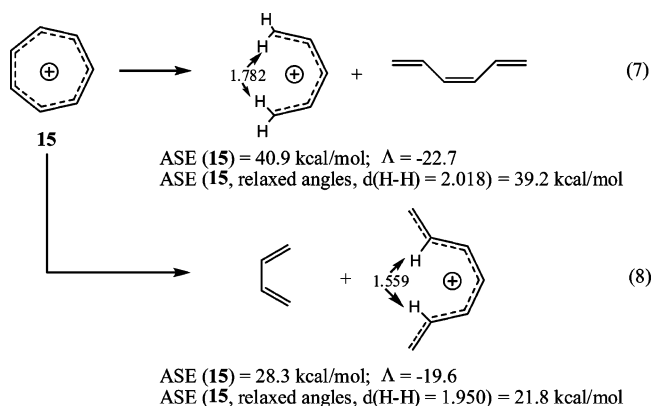
**Models.** Because neither the fragmentation models nor the isomerization models have been, to our knowledge, applied to cationic systems, we sought to evaluate the effects of too little or too much charge delocalization in the models. As a starting point, we applied the more standard approach to determining ASE, namely, eq 5; a similar equation was used to obtain MSE ( $\Lambda$ ) values.

Because tropylium ion (**15**) and **34** are planar with unusual angles and their optimized dihydroaromatics would not be, we chose to constrain all the dihydroaromatics to planarity; the consequent torsional interactions of the saturated C–H bonds would be expected to cancel. However, there remains the problem that the charge delocalization in the aromatic ion is different from that in the dihydroaromatic, and the apparent ASE has to be reduced by an amount corresponding to the diminished charge delocalization in the dihydroaromatic (which makes its energy too high). In other words, the energy change found from eq 5 is really the sum of ASE + CSE (charge stabilization energy). We propose that the appropriate energy correction may be obtained by considering the average charge per  $\pi$  carbon (as judged by Mulliken population analysis) in the aromatic vs the dihydroaromatic. But how can this difference be related to energy? We studied the energy changes for homodesmotic reaction 6. For each set of comparisons (of which only b and d are relevant here; the others are given in the Supporting Information), the energetic effects were only due to the differences in groups attached to the ions (not the neutrals). Contrary to impressions left by valence bond drawings, the charge in these ions is quite delocalized into the alkyl groups (for example, the dipropylpentadienyl cation has 35% of the charge in the alkyl groups), all of which are secondary (the correlation seen below extends to Me and H substituents but becomes fairly qualitative). Figure 1 shows the correlations obtained for going from a pentadienyl to a heptadienyl cation

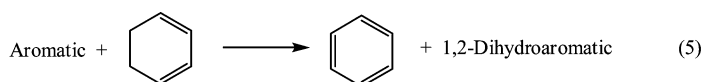
and from a nonatetraenyl to an undecapentaenyl cation. From these correlations of energy change vs average charge/ $\pi$  carbon change, one can calculate that the correction for charge delocalization (i.e., the charge stabilization energy portion of eq 5) is 2.7 kcal/mol in the 7MR case and 1.1 kcal/mol for the planar 11MR case. Using the values for benzene from ref 6, we obtained the derived ASE and MSE values shown. These results suggest that the tropylium ion (**15**) is 3.8 kcal/mol less stabilized by aromaticity than benzene. The best independent estimate for the ASE of **15** is 21.0 kcal/mol, on the basis of the difference in MMP2  $\pi$  energies of **15** and the all-*trans*-1,3,5-heptatrienyl cation (and an ASE of 21.7 kcal/mol for benzene; no similar estimate of  $\Lambda$  is available).<sup>22</sup> The latter value may be flawed because the substitution pattern in the tropylium and model cations is different. Our value is in better agreement with what we obtained via the ISE2 method (see below). The somewhat greater ASE for **34** is not unreasonable.



Next, we applied the fragmentation method to **15**. Because of the small ring size, it was necessary to allow one of the fragments to have some dihedral angles rotated by  $180^\circ$  to avoid very close H–H interactions. The two methods studied are shown in eqs 7 and 8.



It is seen that the MSE values via either method are quite close to the estimates found using eq 5. However, the ASE values given by eq 7 are too high, even when the H–H interactions are removed (by letting the angles increase). This is certainly due to the diminished charge delocalization in the 5C ionic model fragment of eq 7. On the basis of eq 6 for the unsubstituted isomers, the expectation is that the ASE would be too high by 19 kcal/mol, very close to what was calculated. On the other hand, eq 8, for which the 7C ionic fragment has roughly the same charge delocalization as **15**, gives very reasonable ASE values, especially once the H–H nonbonded



$$\text{ASE (Aromatic)} = \text{ASE (benzene)} - E (\text{Aromatic} + \text{cyclohexadiene}) + E (\text{benzene} + 1,2\text{-dihydroaromatic})$$

ASE (Benzene)	= 21.7 kcal/mol	$\Lambda$ (Benzene)	= -13.4
ASE (Tropylium Ion, <b>15</b> )	= 17.9 kcal/mol	$\Lambda$ ( <b>15</b> )	= -23.4
ASE ( <b>34</b> )	= 20.3 kcal/mol	$\Lambda$ ( <b>34</b> )	= -110.4

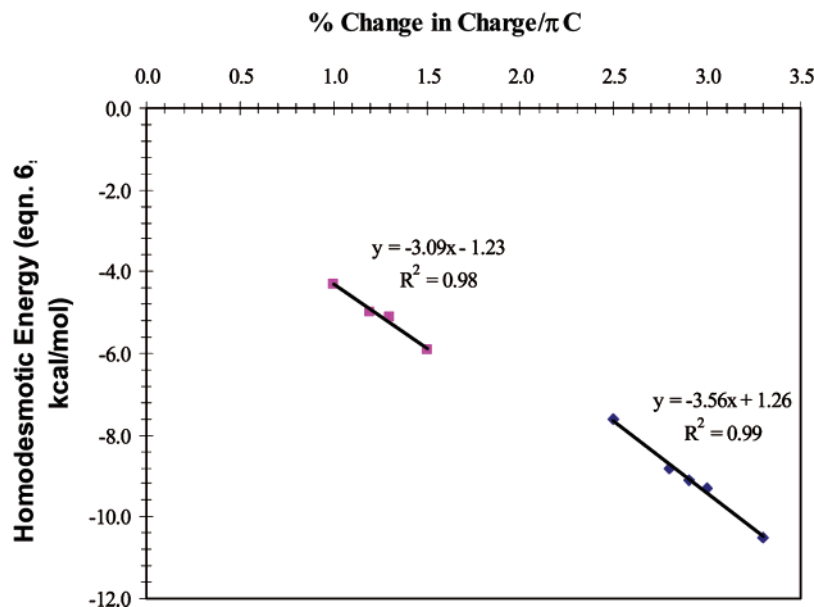


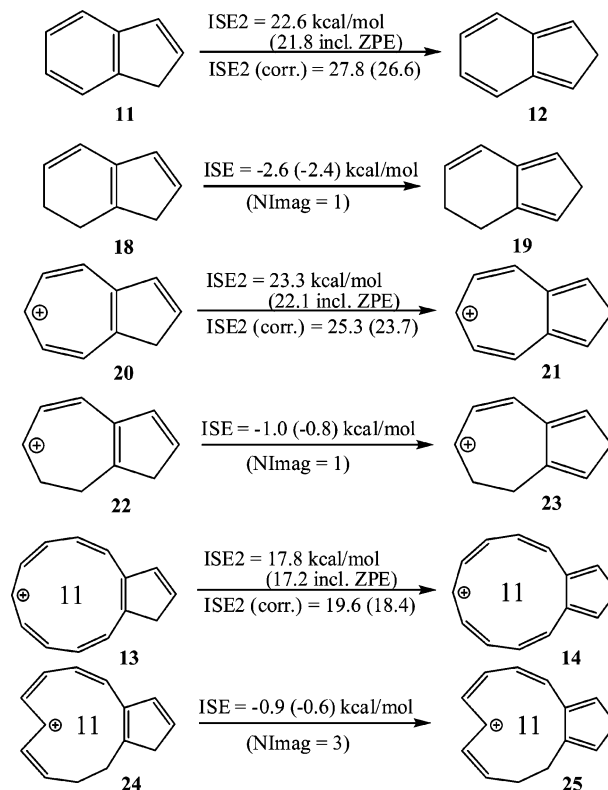
**FIGURE 1.** Plot of case b of eq 6 (pentadienyl to heptadienyl cation (lower right)) and case d of eq 6 (nonatetraenyl to undecapentaenyl cation (upper left)) vs the % change in the average charge per  $\pi$  C (with H charges summed into C).

interaction is accounted for (by allowing the angles to increase). This value is very close to the aforementioned MMP2  $\pi$  results found by Schleyer.<sup>22</sup>

In summary, the MSE values are likely to be reliable independent of the degree of charge delocalization (and magnetic effects are the most reliable indicator of antiaromaticity in larger rings<sup>21</sup>). The ASE values obtained by method B for the 11MR cases are certainly too high, and those obtained by method A are somewhat high (the worst case is probably **34**, where charge delocalization is equalized throughout, and the ASE value is high by about 12 kcal/mol using method A; see Table 2) but not as bad as those for the tropylium ion case (**15**, eq 7) because the difference between charge delocalization from 9 to 11 carbons is much less than that from 5 to 7 carbons (see Figure 1). It is probably best to compare the 11MR cations relative to each other, with the knowledge that **34** has about the same ASE as benzene (eq 5).

**B. Evaluation of the Isomerization Energy II (ISE<sub>II</sub>, ISE2) Model.** The isomerization of indene (**11**) to isoindene (**12**) requires 22.6 kcal/mol (21.8 including ZPE; B3LYP/6-31G\*<sup>22</sup>). Schleyer used a correction of +7.2 kcal/mol because **12** contains two inherently more stable *s-trans*-1,3-butadiene units relative to **11**; the value comes from the energy difference between *s-cis*- and *s-trans*-1,3-butadiene. However, some of that difference is due to the fact that *s-cis*-1,3-butadiene is twisted out of planarity by  $>30^\circ$ , whereas *s-trans*-1,3-butadiene is planar. However, both **11** and **12** are planar. Therefore, a better correction value might be obtained by comparing the energy difference between **18** and **19**, where both have their 6MR held planar (which produces NImag = 1 structures). This leads to a correction of 5.2 kcal/mol (4.8 including ZPE) and a corrected ISE2 value of 27.8 (26.6) kcal/mol for **11**. Similarly, one obtains a corrected ISE2 value for **15** of 25.3 (23.7) kcal/mol, which implies **15** has 2.5 (2.9) kcal/mol less ASE than benzene, which is in accord with

the calculations using eq 5. For the [11]annulenic ion **13**, we have chosen the mono-*trans*-dihydro models **24** and **25** because their optimized bond angles near the ring fusion more closely match those of all-*cis*-**13** than do those of the dihydro all-*cis* structures. We see that the ISE2 approach finds **13** to have less ASE than indene by about 8 kcal/mol, whereas the eq 5 method found very similar ASEs for **34** and benzene.



**C. Monocyclic (C<sub>11</sub>H<sub>11</sub><sup>+</sup>) [11]Annulenic cations.** We were able to locate nine stationary points (see Figure 2).<sup>23</sup> In order of decreasing (B3LYP) stability, these are **26** (the di-*trans* “5+4-

(21) Wannere, C. S.; Moran, D.; Allinger, N. L.; Hess, B. A., Jr.; Schaad, L. J.; Schleyer, P. v. R. *Org. Lett.* **2003**, *5*, 2983.

(22) Reindl, B.; Clark, T.; Schleyer, P. v. R. *J. Phys. Chem. A* **1998**, *102*, 8953.

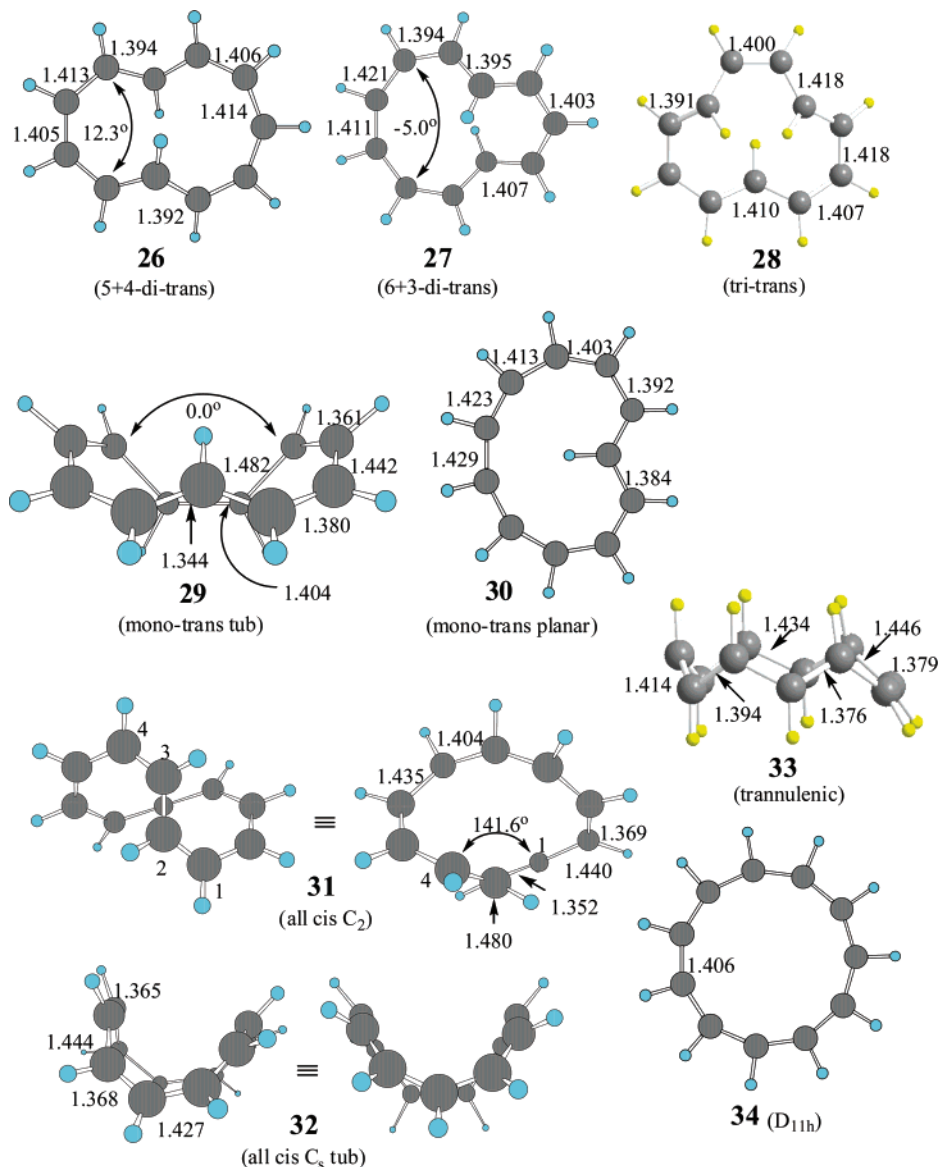
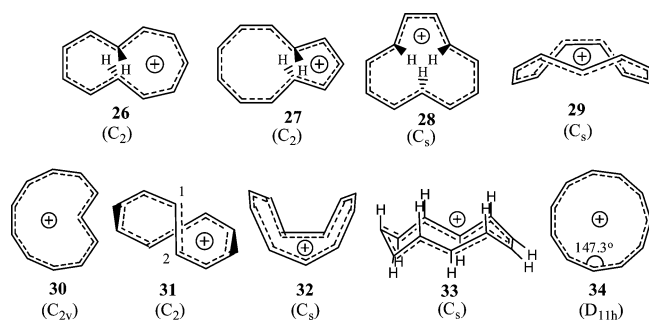


FIGURE 2. 3-D drawings of monocyclic [11]annulanium cation singlet stationary points.

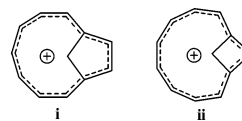
benzotropylium-type”), **27** (the di-*trans* “6+3-azulenic-type”), **28** (the tri-*trans*  $C_s$  structure), **29** (the mono-*trans* tub), **30** (the mono-*trans* planar “heart”), **31** (the all-*cis*  $C_2$  structure), **32** (the all-*cis*  $C_s$  structure), **33** (the “all-*trans*”<sup>24</sup> trannulenic-type<sup>25</sup>  $C_s$  structure), and **34** (the all-*cis* planar structure). As expected, **34**

structure is the transition state for the interconversion of the nonplanar heart structures,<sup>5b</sup> **30** is a second-order saddle point. On the basis of the imaginary frequencies for **30**, we surmise that there is a twisted mono-*trans* structure with one imaginary frequency (that we did not locate). The other six structures (**26**–**29**, **31**, and **33**) are minima.



is not a minimum but rather a second-order saddle point; **32** is the transition state for the interconversion of enantiomeric forms of **31**. Unlike the [10]annulene case, where the planar heart

(**23**) Attempts to derive monocyclic [11]annulanium cations from **i** and **ii** led to **26** and **29**, respectively.



(**24**) It is actually impossible to have an all-*trans* structure for an odd-membered cycle; **33** has the equivalent of five *trans* double bonds.

(**25**) (a) Fokin, A. A.; Jiao, H.; Schleyer, P. v. R. *J. Am. Chem. Soc.* **1998**, *120*, 9364. (b) Wei, X.-W.; Darwish, A. D.; Boltalina, O. V.; Hitchcock, P. B.; Street, J. M.; Taylor, R. *Angew. Chem., Int. Ed.* **2001**, *40*, 2989. (c) Havenith, R. W. A.; Rassat, A.; Fowler, P. W. *J. Chem. Soc., Perkin Trans.* **2002**, *2*, 723. (d) Darwish, A. D.; Kuvytchko, I. V.; Wei, X.-W.; Boltalina, O. V.; Gol'dt, I. V.; Street, J. M.; Taylor, R. *J. Chem. Soc., Perkin Trans.* **2002**, *2*, 1118.

**TABLE 1.** Selected Geometry and Energy Data (kcal/mol) for [11]Annulenicium Cation Stationary Points<sup>a</sup>

compd (singlet)	NImag <sup>b</sup>	$\Delta R_{C-C}$ <sup>c</sup>	Erel <sup>d</sup>	Hrel <sup>d</sup>	Erel <sup>e</sup>	vertical triplet $\Delta E$ (S-T) <sup>d</sup>	optimized triplet $\Delta E$ (S-T) <sup>d</sup>	optimized triplet $\Delta R_{C-C}$ <sup>c</sup>
26	0	2.2	(0.0)	(0.0)	(0.0)	45.3	33.2	9.4
27	0	2.7	4.2	4.3	4.1	54.8	42.8	7.6
28	0	2.7	7.3	7.0	3.7	56.1	42.4	11.0
29	0	13.8	11.1	10.0	5.8	37.6	26.4	4.3
30	2	4.5	20.7	20.6	24.4	58.0		
31	0	12.8	30.4	29.0	27.5	20.8	8.5	2.9
32	1	8.0	32.4	30.9	33.9	31.9		
33	0	7.0	55.7	54.6	50.6	49.8	22.0	7.4
34	2	0.0	61.9	62.4	71.2	57.0		

<sup>a</sup> Structures optimized at B3LYP/6-31G\* (rovibrational corrections at the same level). <sup>b</sup> NImag = number of imaginary frequencies. <sup>c</sup> Difference, in pm, between the shortest and longest C–C bond of the ring. <sup>d</sup> At B3LYP/6-31G\*. <sup>e</sup> At CCSD(T)/6-31G\*\*/B3LYP/6-31G\*.

**TABLE 2.** Aromatic Stabilization Energies (kcal/mol) for [11]Annulenicium Cation Stationary Points Computed by Two Methods

compd (singlet)	26	27	28	29	30	31	32	33	34			
ASE <sup>a</sup>	27.4	21.0	19.0	26.6	3.8	31.2	2.8	6.0	9.0	5.5	32.2	36.4
method	A	A	A	B	A	A	A	B	A	A	A	B
ISE2 <sup>b</sup> (corr.)	15.1	15.2	14.4	4.3	18.0	–4.5	10.5	6.4	19.6			

<sup>a</sup> Aromatic stabilization energy at B3LYP/6-31G\*; for method details, see Computational Methodology and section A of Results and Discussion.

<sup>b</sup> Isomerization stabilization energy approach to ASE evaluation at B3LYP/6-31G\*; for details, see Computational Methodology and section B of Results and Discussion.

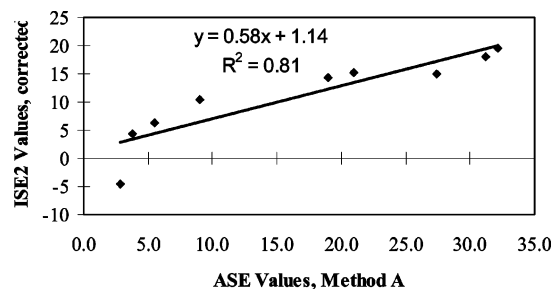
**TABLE 3.** Magnetic Data for [11]Annulenicium Cation Stationary Points

compd	$\chi$ (cgs ppm)			$\Lambda^a$ (method)	NICS (ppm)		av shielding of outer H's (ppm)	
	singlet	vertical triplet	optimized triplet	singlet	singlet	vertical triplet	singlet	vertical triplet
26	–107.0	178.5	–36.5	–44.5 (A)	–16.6	75.4	22.5	32.5
27	–107.0	184.3	–72.8	–41.3 (A)	–13.8	80.6	23.1	32.5
28	–101.0	217.8	–75.8	–48.3 (A) –41.5 (B)	–15.6	98.0	22.7	32.3
29	–67.9	–59.0	–94.0	–11.1 (A)	–2.7	0.3	24.1	23.9
30	–122.0	924.8		–66.6 (A)	–18.8	80.5	21.6	65.0
31	–33.1	–77.8	–88.6	35.2 (A) 28.6 (B)	10.6	–3.8	24.2	24.0
32	–80.8	–41.3		–48.3 (A)	–3.3	6.4	24.0	24.6
33	–90.5	37.6	–89.6	–44.3 (A)	–14.8	33.8	25.9	18.0
34	–134.9	1159.1		–79.9 (A) –77.3 (B)	–13.1	250.5	21.3	72.4

<sup>a</sup> Magnetic susceptibility enhancement (MSE, cgs ppm) based on models according to the given method; for Method details, see Computational Methodology section.

Table 1 presents the relevant geometric and energetic data for **26**–**34**, their vertical triplets (an important measure of electronic structure at the same geometries as the relevant singlets<sup>26</sup>), and their closely related optimized triplets.<sup>26</sup> Table 2 gives a comparison of the ASEs determined by method A (and some by method B) with those obtained by the ISE2 approach. Figure 3 demonstrates the correlation between these two methods (the correlation coefficient rises to 0.93 if the point for **31** is omitted), and Figure 4 shows the specific indene/isindene pair structures used to obtain the ISE2 values. Table 3 presents magnetic data for the monocyclic cations. As might be expected, the inner hydrogens of **26** and **27** point in opposite directions, which makes these ions structurally distinct from **6**. The three inner hydrogens of **28** are unavoidably crowded,

(26) (a) Hückel rules are reversed for the triplet state; the vertical triplet of an aromatic would be the most antiaromatic, whereas the corresponding optimized triplet would be expected to distort so as to reduce the amount of antiaromaticity: Baird, N. C. *J. Am. Chem. Soc.* **1972**, *94*, 4941. (b) For validity of NICS calculations on open-shell systems, including triplets, see: Gogonea, V.; Schleyer, P. v. R.; Schreiner, P. R. *Angew. Chem., Int. Ed.* **1998**, *37*, 1945.

**FIGURE 3.** Correlation between ISE2 and ASE (method A) values for [11]annulenicium ion stationary points (kcal/mol).

although all the data point to it being similar to **26** and **27** in terms of aromaticity.

It is seen that the energetic ordering of all but **28** is the same at the CCSD(T)/6-31G\* level as at the B3LYP/6-31G\* level. As noted for the [10]annulenes, a tendency for B3LYP to overestimate the stability of conjugated species (see **34**) and to underestimate the energy of nonconjugated species (see **29**) relative to what is calculated via the coupled clusters method

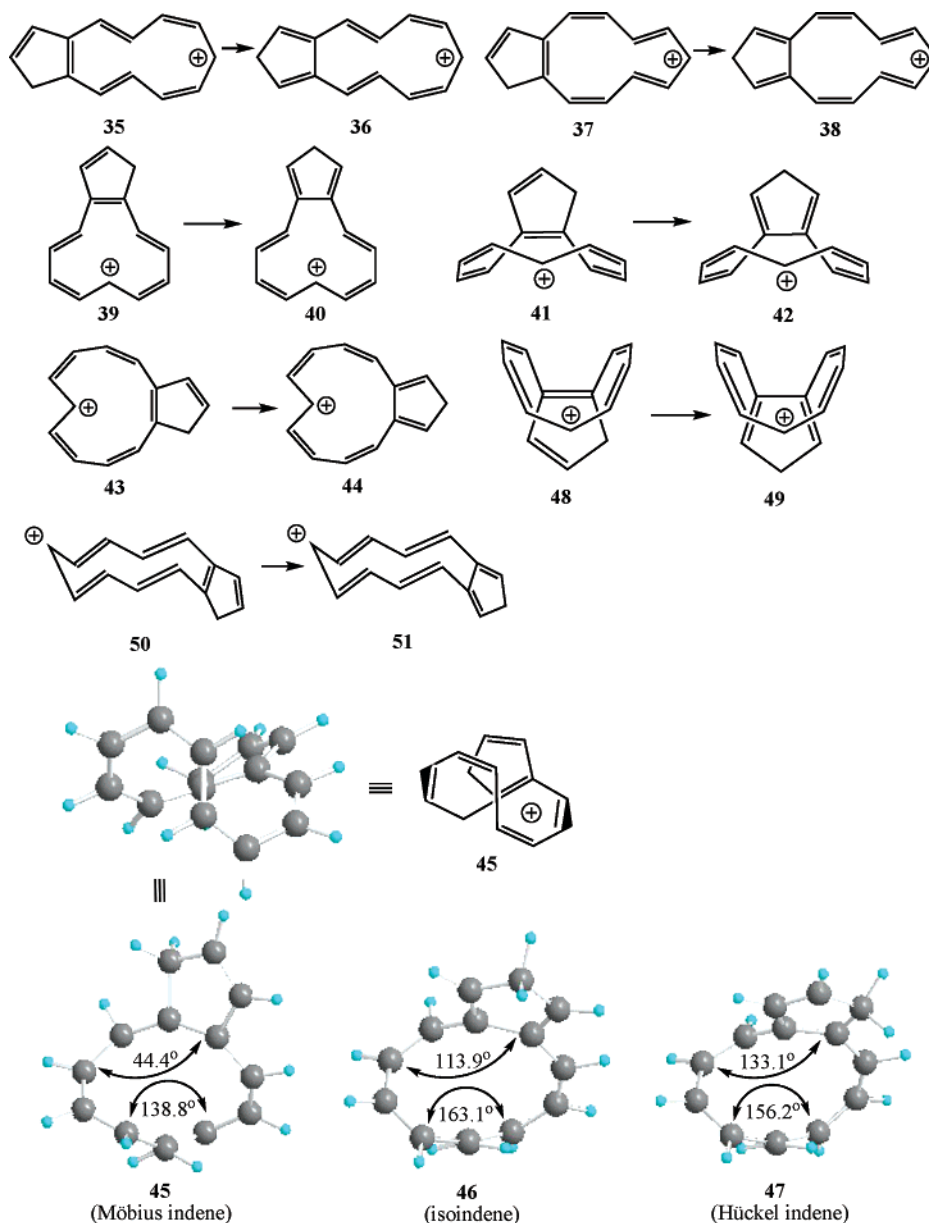


**FIGURE 4.** Structures of the indene/isoindene pairs used to obtain ISE2 values (**13/14** shown earlier). In all but one case, the 5MR fusion is perpendicular to a symmetry plane or axis, so only a single indene is possible. Isomers of **43/44** were also investigated and gave similar results. In the case of antiaromatic **31**, the position of the 5MR fusion was critical. *Except for 45*, all indene fusions led to doubly half-twisted Hückel aromatic systems, of which one (**47**) is shown (see Supporting Information for complete data).

can be observed, but the effect is relatively minor here. The increased stability of **28** at CCSD(T), which is similar to that seen for **29**, but now places it between **26** and **27**, might be largely due to differences in how the two methods handle nonbonded H–H interactions. Perhaps most notably, the energy of minimum **31** is above that of the second-order saddle point **30**. In addition, the singlet–triplet gap (both vertical and optimized) is much smaller for **31** than the other minima. Significant aberrant effects are also seen for the magnetic properties of **31**; these are discussed in a separate section below.

The structures of **26–28**, **30**, and **34** all show the bond equalization (see  $\Delta R_{C-C}$ , Table 1) expected of an aromatic species (**34** was constrained only to be planar via fixing the ring dihedral angles), whereas the tub-shaped minimum **29** and transition state **32** have the alternating bond length sections

expected for noncyclically conjugated carbocations. The optimized triplets (**26t–29t** and **31t**) all show bond alternation that is the opposite of their respective singlets. The ASEs and ISE2s (Table 2) of **26–28**, **30**, and **34** are consistent with aromaticity for these species, with the planar molecules showing somewhat greater aromatic character; the ASEs/ISE2s of **29**, **31**, and **32** are not consistent with aromaticity. The magnetic properties (Table 3) of **26–28**, **30**, and **34** support aromaticity for all five. These include a rather negative magnetic susceptibility ( $\chi$ ) and MSE for the singlet state of each, together with the expected positive (extremely so for **30** and **34**) magnetic susceptibilities for their vertical triplets (which are decidedly antiaromatic); the optimized triplets corresponding to **26** and **27** also show much less negative susceptibilities than the singlets, but they avoid antiaromaticity by twisting out of planarity. A similar trend is



TABLE 4. Some Energetic and Magnetic Data<sup>a</sup> for 3MR-Fused Planar [11]Annulenic Cations and Planar [10]Annulenes

no. fused 3MRs	compd (NImag)	[11]annulenic ions						[10]annulenes					
		ASE <sup>b</sup> (method)		$\chi$		$\Lambda$ (method)	NICS		ASE (method)		$\chi$	$\Lambda$ (method)	NICS
		singlet	singlet	vertical triplet	singlet	singlet	vertical triplet	compd (NImag)	singlet	singlet	singlet	singlet	
0	<b>34</b> (2)	32.2 (A)			-79.9 (A)		<b>2</b> (2)	26.8 (C)	-125.5	-66.2 (C)	-13.6		
		36.4 (B)	-134.9	1159.1	-77.3 (B)	-13.1		250.5	26.1	-182.6 <sup>f</sup>	-80.1	-15.9 <sup>g</sup>	
1	<b>52a</b> (2)	30.4 (A)			-69.5 (A)		<b>57<sup>c</sup></b> (1)	24.0 (C)	-127.1	-59.4 (C)	-13.0		
		36.1 (B)	-133.6	530.0	-66.6 (B)	-12.1		132.1	22.5 (C)	-127.7	-50.1 (C)	-12.5	
2	<b>53a</b> (2)	28.1 (A)			-55.9 (A)		<b>4</b> (0)	13.9	-197.3 <sup>f</sup>	-64.4	-14.9 <sup>g</sup>		
		29.3 (B)	-137.1	285.5	-53.3 (B)	-10.4		93.4	22.0 (C)	-134.4	-46.8 (C)	-11.8	
3	<b>54</b> (0)	29.8 (A)			-54.7 (A)		<b>58<sup>d</sup></b> (0)	24.2 (C)	-139.1	-45.8 (C)	-10.7		
4	<b>55</b> (0)	26.8 (B)	-139.6	162.8	-45.8 (B)	-9.1		68.6	18.3 (C)	-143.4	-37.1 (C)	-9.3	
5	<b>56</b> (0)	26.2 (B)	-145.2	106.2	-41.7 (B)	-8.2	<b>5</b> (0)	18.5	-216.1 <sup>f</sup>	-38.1	-10.8 <sup>g</sup>		
									(ref 6)		(ref 6)		

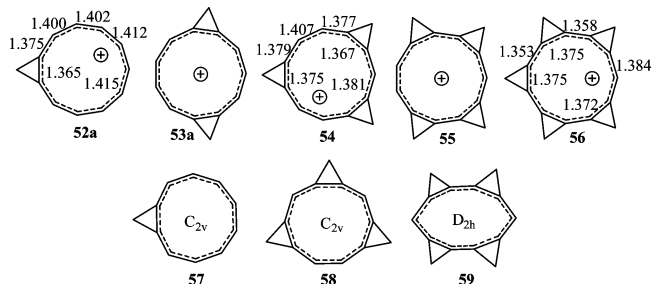
<sup>a</sup> Magnetic susceptibilities ( $\chi$ , cgs ppm) and exaltations ( $\Lambda$ ) from CSGT at B3LYP/6-311+G(d,p)//B3LYP/6-31G(d) and NICS from GIAO at B3LYP/6-31+G(d)//B3LYP/6-31G(d); for method details, see Computational Methodology section. <sup>b</sup> Aromatic stabilization energy at B3LYP/6-31G\*; for Method details, see Computational Methodology section. <sup>c</sup> Although a transition structure, planar cyclopropa[10]annulene (**57**) is lower in enthalpy than the slightly bowl-shaped minimum (**57a**, see Supporting Information). <sup>d</sup> Tricyclopropa[1,2,4,5,7,8][10]annulene, **58** (see Supporting Information for details). <sup>e</sup> Tetracyclopropa[1,2,3,4,6,7,8,9][10]annulene, **59** (see Supporting Information for details). <sup>f</sup> From ref 6: IGLO/DZ//B3LYP/DZ. <sup>g</sup> From ref 6: GIAO at B3LYP/6-31G(d).

seen for the NICS values: -13 to -19 for the aromatic singlets and 75–250 for the antiaromatic vertical triplets. In as much as NICS values are independent of the area of the ring exhibiting a diamagnetic ring current, it is somewhat surprising that the  $D_{11h}$  **34** has the *least* negative NICS of the aromatic species herein; the magnetic susceptibilities and MSEs support *greater* aromaticity for **34** as compared to the other three aromatic structures, and this difference probably reflects local effects on NICS[0].<sup>11c</sup> As in the [10]annulene series, the mono-*trans* planar species (**30**) exhibits strong aromaticity. Interestingly, the average magnetic shielding calculated for the outer H's (see Table 2), which was done using the CSGT/6-311+G\*\* method rather than the GIAO/6-31+G\* method used for the NICS calculations, suggests greater aromaticity for **34** (less shielded, hence more downfield chemical shifted) than the other four aromatic species. The susceptibility and chemical shift calculations indicate the following relative antiaromaticity of the vertical triplets: **34** > **30** > **26**–**28**.

Trannulenic-type isomer **33** is more challenging to characterize. Its  $\pi$  electrons interact cyclically inside and outside the beltlike structure, and pyramidalization of the carbon atoms is evident. This factor may lead to the almost negligible ASE. However, the  $\Lambda$  (-44.3) is substantial, despite a  $\chi$  that is more positive than the other aromatic [11]annulenic cations. Additionally, the NICS (-14.8) value and the  $\chi$  and NICS (33.8) values of the vertical triplet support characterization of **33** as aromatic.

**D. [11]Annulenic Cations Fused to 3MRs.** Schleyer introduced the concept of stabilizing the all-*cis* form of [10]annulene by fusion of two or more 3MRs to the main ring.<sup>6</sup> For example, fusion as in **4** gives a (calculated) planar carbon skeleton. Accordingly, we have studied the fusion of one to five (the maximum) 3MRs around the central all-*cis* 11MR. Although there is only one way to fuse either one or five 3MRs to the central ring (**52** and **56**, respectively), there are four ways to fuse either two or four 3MRs and five ways to fuse three 3MRs. In this section, we discuss the planar (NImag = 2) mono-3MR (**52a**), the planar (NImag = 2) di[1,2:6,7]3MR (**53a**), the symmetrical planar (NImag = 0) tri[1,2:4,5:8,9]3MR (**54**), the

planar (NImag = 0) tetra[1,2:3,4:6,7:8,9]3MR (**55**), and the planar (NImag = 0) penta[1,2:3,4:5,6:7,8:9,10]3MR (**56**) cases.



We also include related all-*cis*, fused [10]annulenes for comparison. (In the next section, we include two additional isomers of **53**, namely, **63** and **64**, which are related to **31**.) Table 4 gives relevant data for the aforementioned fused systems.

It is apparent, especially from the MSE ( $\Lambda$ ) and NICS data, that the aromaticity of the planar species (and antiaromaticity of the vertical triplets) diminishes as additional 3MRs are fused around the central [11]annulenic cation; the ASE data show the same trend, except for with **53a** or **54** (one of these is slightly out of order, but both fall between **52** and **55**).

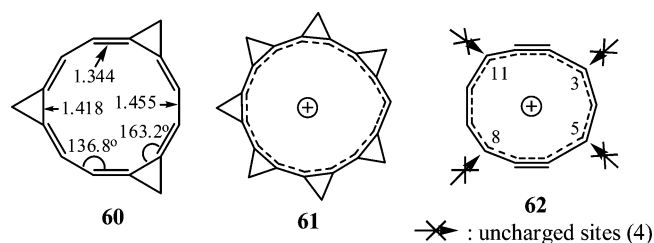
Our ASE and magnetic data for the [10]annulenes show the same effect for 3MR fusion (where our data enlarge on the trend already apparent in the report by Schleyer<sup>6</sup>); the numerical differences between ours and Schleyer's  $\chi$  and NICS data for the [10]annulenes are due to the use of different basis sets and/or calculation algorithms. It is noteworthy that our ASE results compare well to Schleyer's, except for those for **4** (where his result does not fit the trend for the rest of his data); a comparison of  $\Lambda$  results shows agreement, except that again Schleyer's result for **4** is out of line with respect to the other 3MR fused cases. Of interest is that although planar monocyclopropa[10]annulene, **57**, is a transition state, it is actually 0.5 kcal/mol lower in *enthalpy* than its related slightly bowl-shaped minimum (**57a**, see Supporting Information for details). (It is commonly observed that the enthalpy of a minimum will rise above that of a related

**TABLE 5.** Selected Geometric (B3LYP/6-31G\*), Energetic, and Magnetic Data<sup>a</sup> for Möbius [11]Annulene Ions and, for Comparison, Three Related Twisted Species

species (sym)	CC <sub>1</sub> C <sub>2</sub> C <sup>b</sup>	ΔR <sub>C-C</sub> <sup>c</sup>	R <sub>1-2</sub> <sup>d</sup>	ASE <sup>e</sup> (method)	χ	Λ (method)	NICS <sup>f</sup>
<b>31</b> (C <sub>2</sub> )	141.6°	12.8	1.480	2.8 (A) 6.0 (B)	-33.1	35.2 (A) 28.6 (B) <b>31-vt</b> <sup>g</sup>	10.6
-77.8	-3.8						
<b>31t</b> (C <sub>2</sub> )	161.4°	2.9	1.407		-88.6 48.6		-8.6 39.3
<b>31t-vs</b> <sup>g</sup>							
<b>52b</b> (C <sub>1</sub> )	144.3°	12.4	1.471	4.9 (A) 5.0 (B)	-49.3	26.5 (A) 21.5 (B) <b>52b-vt</b> <sup>g</sup>	6.8
-87.3	-4.6						
<b>52t</b> (C <sub>1</sub> )	172.3°	4.9	1.396		-98.8 38.3		-10.2 32.1
<b>52t-vs</b> <sup>g</sup>							
<b>63</b> (C <sub>2</sub> )	78.8°	7.9	1.442	29.2 (A)	-111.1	-32.7 (A)	-6.0
<b>63-vt</b> <sup>g</sup>					32.9		28.8
<b>63t</b> (C <sub>2</sub> )	173.4°	3.6	1.386		-106.2 12.5		-8.5 32.2
<b>63t-vs</b> <sup>g</sup>							
<b>64</b> (C <sub>1</sub> )	129.5°	6.5	1.423	13.2 (A) 35.1 (B)	-101.2	-36.2 (A) -23.9 (B) <b>64-vt</b> <sup>g</sup>	-8.4
-31.8	15.2						
<b>64t</b> (C <sub>1</sub> )	175.7°	6.2	1.392		-106.4 13.5		-8.9 32.1
<b>64t-vs</b> <sup>g</sup>							
[9]annulene cation (C <sub>2</sub> )	141.8°	3.9 <sup>h</sup> 4.3 <sup>k</sup>	1.425	17.1 (E)	-70.0	-22.8 (E) <sup>i</sup> -18.8 <sup>k</sup>	-10.8 <sup>j</sup> -13.4 <sup>k</sup>
[9]annulene cation-vt <sup>g</sup>	-68.0		44.5				
[10]annulene (C <sub>2</sub> )	91.1°	14.2	1.481	1.4 (C)	-63.7	1.3 (C)	2.8
[10]annulene-vt <sup>g</sup>					-68.2		-0.6
[12]annulene (D <sub>2</sub> )	158.4°	10.4	1.453	-5.8 (D)	-88.9 <sup>l</sup>	-10.3 (D)	-8.0
[12]annulene-vt <sup>g</sup>					-72.6		4.7

<sup>a</sup> Magnetic susceptibilities (χ, cgs ppm) and exaltations (Λ) from CSGT at B3LYP/6-311+G(d,p)/B3LYP/6-31G(d) and NICS from GIAO at B3LYP/6-31+G(d)/B3LYP/6-31G(d); for method details, see Computational Methodology section. <sup>b</sup> Main ring dihedral angle that is most deviant from 0° or 180° and is responsible for the Möbius twist. <sup>c</sup> Difference, in pm, between the shortest and longest C–C bond of the main ring. <sup>d</sup> The bond distance (Å) around the twisted portion of the ring (see dihedral angle definition in column 2); this is the longest or near longest ring bond in the singlets. <sup>e</sup> Aromatic stabilization energy at B3LYP/6-31G\*; for Method details, see Computational Methodology section. <sup>f</sup> These values are at the rough center of the ring, with the ghost atom positioned midway between C<sub>1</sub> and C<sub>2</sub>, and correspond to “NICS[0]”. <sup>g</sup> “vt” stands for vertical triplet of the given singlet species, whereas “vs” stands for “vertical singlet” of the optimized triplet species (in these cases, slightly lower in energy than the triplet). <sup>h</sup> The difference between this value and the published value is due to the use of different basis sets for the optimizations. <sup>i</sup> The published value was determined by reference to the C<sub>s</sub> transition structure that is essentially a planar pentadienyl cation with two nonconjugated double bonds and a NICS = -0.9; the agreement with the model-based value determined here is noteworthy. <sup>j</sup> The difference between this value and the published value is probably due to the exact location of the ghost atom; for example, we find that, at 1 Å away from the point that gave the value above, NICS rises to -12.6. <sup>k</sup> Data from ref 33. <sup>l</sup> The difference between this value and the published value<sup>11c</sup> (-83.3) is likely due to the different basis sets used to perform the calculations.

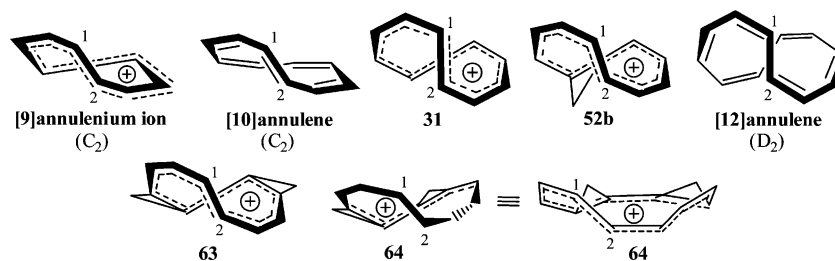
transition state due to the loss of some vibrational energy in the latter, when the barrier in question is very low. In effect, the energy surface becomes very flat across the geometric variable in question, which, in this case, is going from a nonplanar bowl to a planar bowl to the inverted nonplanar bowl.) On the other hand, the planar monocyclopropa[11]annulene ion (**52a**) lies 24.0 kcal/mol higher in enthalpy than its stereoisomeric twisted minimum (**52b**). The planar dicyclopropa[11]annulene ion **53a** also lies above its related bowled minimum, **53b**, but by only 2.6 kcal/mol in enthalpy. Thus, although only one fused 3MR is sufficient to planarize all-*cis*-[10]annulene, it takes three 3MRs to planarize the all-*cis*-[11]annulene cation.



We also found that tricyclopropa[1,2:5,6:9,10][12]annulene (**60**) is a planar, *D*<sub>3h</sub> (internal angles of 136.8° and 163.2° vs 150° in the hypothetical *D*<sub>12h</sub> structure), R stable, *antiaromatic*, all-*cis*-[12]annulene derivative [ASE = -0.6 kcal/mol (method D), Λ = 118.9 (method D), χ = 18.6, χ<sup>vertical triplet</sup> = -176.9,

χ<sup>opted nonplanar triplet</sup> = -180.3, χ<sup>opted planar triplet</sup> = -181.4; NICS = 24.4, NICS<sup>opted nonplanar triplet</sup> = -12.9; ΔE(S–T) = 8.9 kcal/mol, singlet lower at B3LYP/6-31G(d)].<sup>27</sup> The planar, *D*<sub>3h</sub> triplet has NImag = 2 but is 1.1 kcal/mol below the slightly bowled, nonplanar triplet minimum in enthalpy (see Supporting Information for details). The case of the heptacyclopropa[15]annulene cation (**61**) is also interesting. The aromatic planar species [ASE = 15.5 kcal/mol (method F), Λ = -99.3 (method F), χ = -245.8, χ<sup>vertical triplet</sup> = 187.1] has NImag = 2 (14i, 10i), but the slightly twisted C<sub>2</sub> minimum (**61a**, χ = -243.5) is actually 1.0 kcal/mol higher in enthalpy. The planar species has little bond alternation (ΔR<sub>C-C</sub> = 3.5 pm) and accommodates the angular demands with internal C–C angles that range from 154.4° to 162.1° around the fused 3MR junctions and are 133.4° at the lone unfused site (a *D*<sub>15h</sub> structure would have 156° internal angles). Thus, it appears possible to produce a planar, aromatic, all-*cis*-[15]annulene cation derivative.<sup>28</sup>

(27) A reviewer expressed concern that the antiaromatic singlet species (e.g., **31**, **52b**, **60**), although R stable (i.e., stable with respect to becoming unrestricted, diradical-like species) at the DFT level, would actually be multiconfigurational species and thus not treated correctly by B3LYP. To evaluate this, we carried out CAS(10,11)SCF/6-31G\* calculations on **31** and **52b** and a CAS(12,12)SCF/6-31G\* calculation on **60**. The resulting (c<sub>1</sub>/c<sub>2</sub>)<sup>2</sup> values are 106.7, 102.5, and 44.3. These indicate that the wave functions are adequately described by a single configuration. Contrariwise, square planar cyclobutadiene has a (c<sub>1</sub>/c<sub>2</sub>)<sup>2</sup> value of 1.0 at CAS(4,4)SCF/6-31G\*, which indicates its diradical, multiconfigurational nature and suggests the molecule would undergo Jahn–Teller distortion (to rectangular cyclobutadiene).



Finally, in analogy to 1,6-didehydro[10]annulene,<sup>29</sup> we found that the 1,6-didehydro[11]annulenic cation (**62**) is also aromatic [ASE = 47.8 kcal/mol (method A),  $\Lambda = -64.7$  (method A),  $\chi = -111.7$ , NICS =  $-14.0$ ]. For the [10]annulene analogue, ASE suggested less, but NICS suggested greater aromaticity than the other planar cases considered.<sup>6</sup> For **62**, ASE and NICS indicate greater aromaticity than all other [11]-annulenic cations studied, but  $\Lambda$  puts it between **52a** and **53a**. At least for NICS, the value might be enhanced due to the in-plane  $\pi$  electrons in **62**. As shown in the diagram, there is essentially no charge at C<sub>3</sub>, C<sub>5</sub>, C<sub>8</sub>, and C<sub>11</sub>; the other seven carbons share the charge fairly evenly (Mulliken analysis). This means that resonance forms that place the charge adjacent to a triple bond do not contribute, presumably due to the poor conjugative ability of the triple bond.<sup>30</sup>

**E. All-cis-[11]Annulenic Ions are Möbius Antiaromatic Species.** Heilbronner's<sup>31</sup> 1964 postulation of "Möbius aromaticity" has had its greatest success as a transition-state concept, as elaborated by Zimmerman.<sup>32</sup> Schleyer's<sup>33</sup> 1998 computation of the most stable conformation (nonplanar C<sub>2</sub>) of the cyclononatetraenyl cation ([9]annulenic cation) led to the assignment of this ion as a Möbius aromatic species on the basis of a relatively negative NICS ( $-13.4$ ), an apparent substantial MSE ( $-18.8$ ), and relatively small bond alternation ( $\Delta R_{C-C} = 4.3$  pm). More recently, Castro et al.<sup>11a</sup> have found that although the lowest-energy conformation (nonplanar, doubly half-twisted, D<sub>2</sub>) of all-cis-[12]annulene is nonaromatic (NICS,  $-8.1$ ; MSE,  $-18.3$ ;  $\Delta R_{C-C}$ , 10.3 pm) a 4.7 kcal/mol higher C<sub>1</sub> species has the properties of a Möbius aromatic (NICS,  $-14.6$ ; MSE,  $-36.5$ ;  $\Delta R_{C-C}$ , 7.8 pm). These authors also found evidence for Möbius aromaticity in some conformers of [16]- and [20]annulene. A Möbius [16]annulene has been prepared<sup>34</sup> but appears to be nonaromatic.<sup>35</sup> To our knowledge, there have been no instances of Möbius antiaromaticity suggested for ground-state molecules.

Some geometric and magnetic data for **31**, cyclopropa[11]-annulenic cation **52b**, dicyclopropa[11]annulenic cations **63**

and **64**, and their relevant triplets are given in Table 5; also included for comparison are data for the aforementioned C<sub>2</sub> [9]-annulenic cation, C<sub>2</sub> [10]annulene, and D<sub>2</sub> [12]annulene. As originally discussed, the [9]annulenic cation has a Möbius twist, with curtailed orbital interaction at the twist point (dihedral angle of 141.8°, or 38.2° short of ideal). The new data here are somewhat conflicting: the vertical triplet shows a magnetic susceptibility ( $\chi$ ) only 2 units more positive than the singlet, which is not really consistent with aromaticity. However, sometimes strange effects are seen for triplet susceptibilities. The rather large, positive NICS value of 44.5 is reassuring for the assignment of reasonable Möbius aromaticity to the [9]annulenic cation, as is the similarity between our model-based  $\Lambda$  value and the one based on a nonaromatic [9]annulenic cation isomer (Table 5).<sup>32</sup> The C<sub>2</sub> [10]annulene global minimum has bond alternation and magnetic properties consistent with polyenic character; the roughly 90° dihedral around the most twisted bond prevents cyclic delocalization. Its vertical triplet confirms these properties. The D<sub>2</sub> all-cis-[12]annulene global minimum, as discussed before, also has bond and magnetic properties consistent with polyenic character (it has two twists of 158.4° each); its vertical triplet shows only somewhat more positive  $\chi$  and NICS values, also consistent with polyene character.

The [11]annulenic cations show variation that is a function of the number and position of any fused 3MRs (as already seen for the 5MR indene fusions; Figure 4). The parent, **31**, has the largest difference in maximum and minimum ring bond lengths ( $\Delta R_{C-C} = 12.8$  pm), a much more positive  $\chi$  ( $-33.1$ ) than any of its stereoisomers, and a positive  $\Lambda$  (35.2, method A) and NICS (10.6). The sense that this structure is antiaromatic is supported by the more negative  $\chi$  ( $-77.8$ ) and NICS ( $-3.8$ ) found for its vertical triplet (**31-vt**), which shows the requisite (relatively) aromatic properties. The ASE value of 2.8 kcal/mol (method A) is slightly greater than that for the C<sub>2</sub> [10]-annulene but would become negative if charge delocalization were properly accounted for in the model; witness the negative ISE2 value for **31** ( $-4.5$  kcal/mol). As expected, the optimized triplet, **31t**, twists more (dihedral of 161.4°) to achieve better  $\pi$  overlap and undergoes bond equalization ( $\Delta R_{C-C} = 2.9$  pm) to achieve more aromaticity, as evidenced by the more negative  $\chi$  ( $-88.6$ ) and NICS ( $-8.6$ ). Also, the vertical singlet of **31t** is dramatically more antiaromatic than **31** ( $\chi = 48.6$ ; NICS = 39.3) and is a spin-unrestricted species ( $S^2 = 1.1$ ). Cyclopropa[11]-annulenic cation **52b** shows exactly parallel behavior to **31**; this also includes the properties of its optimized triplet, **52t**, and the relevant vertical triplet and singlet species (Table 5 and illustration).

Very different properties are seen for dicyclopropa[11]-annulenic cations **63** and **64**. With a  $\chi$  of  $-101.2$  and a NICS of  $-8.5$ , **64** appears to have aromatic character. Inspection of the structure shows it has two twists (129.5° and  $-117.0^\circ$ ), which makes it a Hückel system, but it is nonplanar and tub shaped. However, the ASE and  $\Lambda$  values also suggest at least

(28) For a bisdehydro[15]annulenic cation, see: Howes, P. D.; Sondheimer, F. *J. Am. Chem. Soc.* **1972**, *94*, 8261. For a bridged [15]annulenic cation, see: Oagawa, H.; Shimojo, N.; Kato, H.; Saikachi, H. *Tetrahedron* **1974**, *30*, 1033.

(29) (a) Myers, A. G.; Dragovich, P. S. *J. Am. Chem. Soc.* **1993**, *115*, 7021. (b) Myers, A. G.; Finney, N. S. *J. Am. Chem. Soc.* **1992**, *114*, 10986. (c) Sondheimer, F. *Proc. Robert A. Welch Found. Conf. Chem. Res.* **1968**, *12*, 125.

(30) Rogers, D. W.; Matsunaga, N.; McLafferty, F. J.; Zavitsas, A. A.; Liebman, J. F. *J. Org. Chem.* **2004**, *69*, 7143.

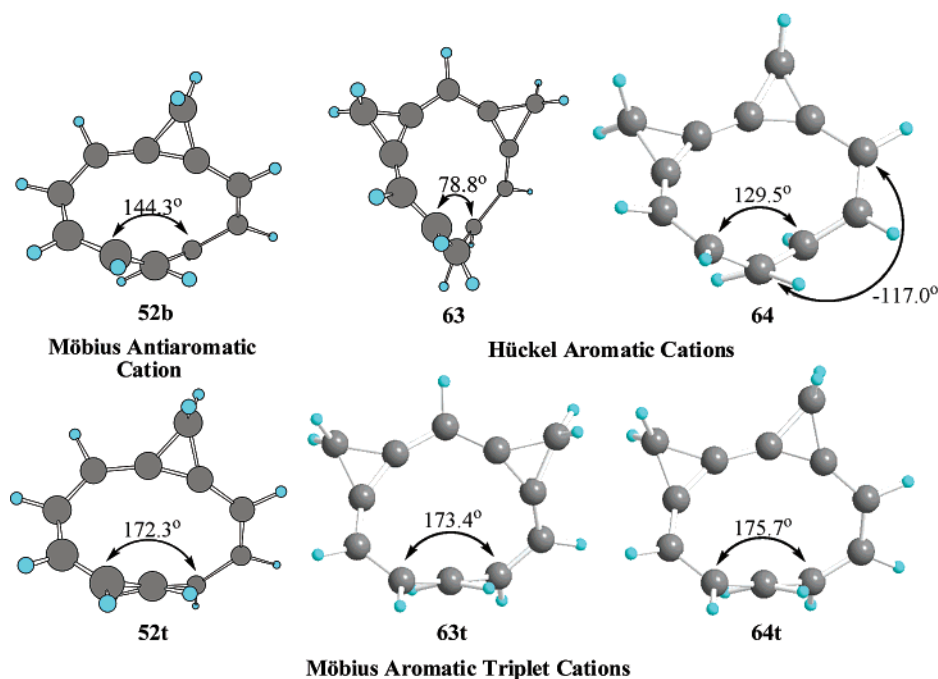
(31) Heilbronner, E. *Tetrahedron Lett.* **1964**, 1923.

(32) (a) Zimmerman, H. E. *Acc. Chem. Res.* **1971**, *4*, 272. (b) Zimmerman, H. E. *J. Am. Chem. Soc.* **1966**, *88*, 1564.

(33) Mauksch, M.; Gogonea, V.; Jiao, H.; Schleyer, P. v. R. *Angew. Chem., Int. Ed.* **1998**, *37*, 2395.

(34) Ajami, D.; Oeckler, O.; Simon, A.; Herges, R. *Nature* **2003**, *426*, 819.

(35) Castro, C.; Chen, Z.; Wannere, C. S.; Jiao, H.; Karner, W. L.; Mauksch, M.; Puchta, R.; Hommes, N. J. R. v. E.; Schleyer, P. v. R. *J. Am. Chem. Soc.* **2005**, *127*, 2425.



some aromatic character (this is the case with the most variation of ASE and  $\Lambda$  depending on the models used; see Table 5). The  $\chi$  and NICS values calculated for the vertical triplet are not sufficiently positive to attribute more than some aromaticity to **64**. It must be pointed out that the inter- $\pi$ -type orbital angles around the twists are only about  $50^\circ$  from the ideal alignment, thereby allowing for beneficial conjugation. Isomer **63** has an even more negative  $\chi$ , a more positive ASE, and much more positive  $\chi$  and NICS values for the vertical triplet. Yet **63** has one twist of  $78.8^\circ$  (less than the  $>90^\circ$  required to be Möbius), which should eliminate cyclic aromatic conjugation. Close inspection of the twisted region, however, shows that the central two carbons are significantly *antipyramidalized* (unlike the [10]-annulene discussed above, which is essentially unpyramidalized). This produces an inter- $\pi$ -type orbital angle of  $61.4^\circ$ , rather than the  $78.8^\circ$  implied by the dihedral angle (Table 5). Although still not ideal for aromatic overlap, this angle appears to be sufficient to allow some ordinary aromatic interaction (note that the magnetic effects are much smaller than in the planar isomer **53a**).

The optimized triplets of **63** and **64** (**63t** and **64t**) are clearly  $10\pi$  electron Möbius aromatic systems with nearly ideal dihedral angles around the twist (note that **64t**, unlike **64**, has only one twist). Their corresponding vertical singlets (as is the case for the analogous **31t-vs** and **52t-vs**, **63t** and **64t** are unrestricted species) are, as expected, antiaromatic (on the basis of both  $\chi$  and NICS; Table 5).

The obvious question is why would **31** and **52b** adopt *antiaromatic* structures as their most stable conformations? The answer must lie in the overall conformational energy of these unsaturated medium rings. The shapes of the [9]annulene, [10]annulene, **31**, **52b**, and [12]annulene rings are all quite similar, which suggests these structures are primarily driven by conformational considerations, with aromatic effects as a relatively small add-on to these. The increased conjugation in the [11]annulene cations, which leads to antiaromaticity, as compared to the lack thereof in [10]annulene, is probably due to the benefits of additional charge delocalization in the cations.

The completely different properties of the dicyclopropa[11]-annulene cations **63** and **64**, as well as the differences between apparently similar 5MR-fused indene-type derivatives (**45** and **47**), attest to the subtlety of these conformational effects in medium rings (note that the two  $>90^\circ$  twists in **64** and **47** are located at different spots around the 11MR).

## Conclusions

We have theoretically investigated monocyclic [11]annulene cations and related derivatives with fused 3MRs. For the parent ions, six minima have been identified. In order of decreasing (B3LYP) stability, these are: di-*trans*-**26** (benzotropylium-like), di-*trans*-**27** (azulene-like), tri-*trans*-**28** ( $C_s$ ), mono-*trans*-**29** (tub shaped), all-*cis*-**31** ( $C_2$  twisted), and penta-*trans*-**33** (trannulenic  $C_s$ ); at CCSD(T), **27** and **28** switch places. Although the first three and **33** all have aromatic properties, **29** is nonaromatic, and **31** is a Möbius *antiaromatic* molecule. The maintenance of an antiaromatic structure is attributed to general conformational effects in medium rings of this size. Fusion of one 3MR to **31** (to give **52b**) also results in a Möbius antiaromatic structure.

Fusion of one or two 3MRs to **31** is not sufficient to enforce planarity; three 3MRs, distributed as in **54**, are necessary to produce a planar 11MR minimum. For the all-*cis*, all-planar species (minima and saddle points), fusion of 3MRs sequentially diminishes the apparent degree of aromaticity. There appears to be no reason these cations could not be synthesized.

**Acknowledgment.** This work benefited from the allocation of supercomputer time on the HP rx2600 Itanium2 HP-UX research computing cluster at Northeastern University's Advanced Scientific Computation Center (ASCC).

**Supporting Information Available:** Coordinates and energies for all previously unreported structures discussed herein. This material is available free of charge via the Internet at <http://pubs.acs.org>.

JO061143S